The Moist Available Energy of a Conditionally Unstable Atmosphere

DAVID A. RANDALL AND JUNYI WANG

Department of Atmospheric Science, Colorado State University, Fort Collins, Colorado

(Manuscript received 16 October 1990, in final form 1 July 1991)

ABSTRACT

The concept of "moist available energy," defined by Lorenz, is applied to study the potential energy available for cumulus convection in a conditionally unstable atmosphere. A modified version of Lorenz's parcel-moving algorithm is applied to the GATE data to determine the time variations of the moist available energy of the observed tropical atmosphere. Lorenz's algorithm is found to be somewhat impractical, and a new algorithm based on mass exchanges is proposed. Implications for cumulus parameterization are discussed.

1. Introduction

Conditional instability is a concept that is familiar to every first-year meteorology student. The methods that are used to detect conditional instability in observed or simulated soundings typically involve consideration of the potential energy that can be released when a parcel is displaced vertically. The parcel's level of origin is usually chosen somewhat arbitrarily, and the possibility of multiple parcels originating at multiple levels is usually not admitted. The response of the parcel's environment is usually not taken into account.

We need a method to determine the potential energy available for cumulus convection without such restrictive and arbitrary assumptions. The purpose of this paper is to show that Lorenz's (1978) concept of "moist available energy" holds the key to such a method.

Lorenz (1955) defined the available potential energy (APE) of the atmosphere as the difference between the actual total enthalpy and the minimum total enthalpy that could be achieved by rearranging the mass under reversible adiabatic processes.

This definition can be understood by considering the conservation equation for the total energy of the atmosphere (including the internal, potential, and kinetic energies). According to this equation, the sum of the kinetic energy per unit mass and the enthalpy per unit mass changes in time due to redistribution of mass within the atmosphere, and also due to energy sources and sinks such as radiation, latent heating, and surface exchanges. Here the enthalpy per unit mass is defined as the product of the temperature and the specific heat at constant pressure. Of course, when the total energy equation is integrated over the entire atmosphere, the redistribution term drops out. In the absence of energy sources or sinks, therefore, we find that

$$\frac{\partial}{\partial t}(K + H) = 0, \tag{1.1}$$

where K is the total kinetic energy, and H is the total enthalpy.

The total enthalpy can be varied by adiabatically redistributing mass over the globe, and Lorenz pointed out that there exists a particular mass distribution for which H is minimized. According to (1.1), K is maximized for this same state, which Lorenz called the *reference state*. The APE is then defined as the difference between the total enthalpy of the given state and that of the reference state. It thus represents the portion of the nonkinetic energy that is available for conversion into kinetic energy under reversible adiabatic processes.

Lorenz (1978, 1979; hereafter L78 and L79, respectively) extended the concept of APE to the moist atmosphere by recognizing that moist adiabatic processes are, in fact, adiabatic rather than diabatic. From this point of view, the latent heat of water vapor is a portion of the enthalpy. He presented both graphical and digital algorithms for determining the moist available energy. The latter was based on rearranging discrete parcels from their configuration in the given state to that in the reference state. He showed that the moist available energy (MAE) is never less than the dry available energy (DAE, synonymous with the dry APE), although the DAE represents the bulk of the total available energy in the global atmosphere. He demonstrated that for fixed relative humidity the MAE increases rapidly as the temperature increases. He was also able to define a specific MAE, i.e., the contribution of a particular parcel to the global MAE. The fact that the MAE is an

Corresponding author address: Dr. David A. Randall, Department of Atmospheric Science, Colorado State University, Fort Collins, CO 80523.

upper bound on the amount of kinetic energy that can be generated by any circulation whatsoever is both a strength and a weakness. It is a strength because the concept is completely general. It is a weakness because it is possible that no dynamically realizable circulation can extract all of the available energy.

The concept of available energy is usually applied to statically stable atmospheric states, but it is equally applicable to statically unstable systems. When the atmosphere is everywhere statically stable in the dry sense, the DAE is entirely due to the existence of temperature gradients along isobaric surfaces, i.e., the DAE resides in the horizontal rather than the vertical structure of the atmosphere. The reference state can be reached by rearranging the mass of the system so that the pressure is uniform along isentropic surfaces. The vertical ordering of the isentropic surfaces does not change during this process. For a dry statically unstable system, on the other hand, the reference state can only be reached by vertically reordering the isentropes; the potential temperature decreases upward in the given state, but increases upward in the reference state.

As an example, consider a simple system containing two parcels of equal mass. In the given state, parcels with potential temperatures θ_1 and θ_2 reside at pressures p_1 and p_2, respectively. We assume that $\theta_1 < \theta_2$ and $p_1 < p_2$, so that the given state is statically unstable. The enthalpy per unit mass of parcel i is $c_p\theta_i(p_i/p_0)^\kappa$, where p_0 is the reference pressure used in the definition of the potential temperature, and κ is Poisson's constant. If the parcels are interchanged ("swapped") so that parcel number 2 goes to pressure p_1 and vice versa, the change in the total enthalpy per unit mass is $c_p(\theta_1 - \theta_2)[(p_2/p_0)^\kappa - (p_1/p_0)^\kappa]$, which is negative. This implies that the total enthalpy is minimized by the swap; the final state is the reference state, and the change in enthalpy given above is the available potential energy of the system.

The moist atmospheres used as examples in L78 and L79 were statically stable everywhere; for such atmospheres, the MAE resides in the horizontal rather than the vertical structure. Lorenz did point out, however, that the existence of conditional instability represents a supply of MAE and complicates the design of algorithms to determine the MAE. Consider an idealized atmosphere that is horizontally homogeneous but conditionally unstable. Since the dry static stability is positive, the DAE is zero, but the MAE is positive. When the given state is conditionally unstable, a portion of the air in the reference state must be saturated.

Of course, the real atmosphere is horizontally inhomogeneous and contains local regions of conditional instability. The MAE of the real atmosphere resides, therefore, partly in the atmosphere's horizontal structure and partly in its vertical structure. For convenience, we say that the MAE has both horizontal and vertical "components." The vertical component of the MAE is a generalization of the convective available potential energy (CAPE); to distinguish it from Lorenz's globally defined MAE, we refer to the local vertical component of the MAE as the generalized CAPE, or GCAPE.

The GCAPE is converted into the kinetic energy of cumulus convection on the relatively fast time scale of the convection itself—on the order of an hour or at most a few hours (e.g., Lord and Arakawa 1980; Soong and Tao 1980; Krueger 1988; Dudhia and Moncreif 1988; Xu 1991). As a result, the convectively active atmosphere never strays far from conditional neutrality (e.g., Arakawa and Schubert 1974; Xu and Emanuel 1987); the GCAPE is consumed as rapidly as it is generated by such processes as large-scale rising motion, radiative cooling, moisture convergence, and surface evaporation. In contrast, the horizontal component of the MAE is inaccessible to cumulus convection but can be released by such relatively slow mechanisms as baroclinic instability, with time scales on the order of a few days.

In short, there is a great difference in time scale between the cumulus circulations that draw on the GCAPE and the synoptic circulations that draw on the horizontal component of the MAE. Because of this scale separation, it is useful to distinguish between the horizontal and vertical components of the MAE. In particular, *the dynamical processes that tend to increase or decrease the GCAPE can be considered separately from those that tend to increase or decrease the portion of the available potential energy that resides in the horizontal structure of the atmosphere.* In a sense, this is a basic premise of all cumulus parameterization the-

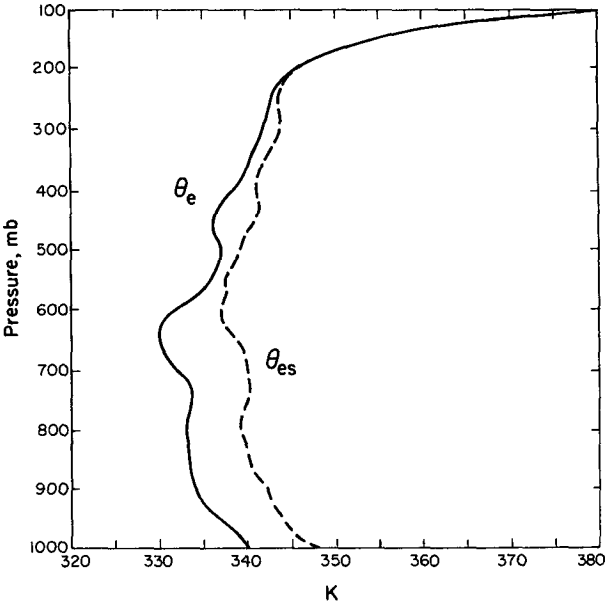

FIG. 1. Observed soundings of equivalent potential temperature (solid line) and saturation equivalent potential temperature (dashed line) for GATE Phase III, 1800 UTC 30 August.

ories (Arakawa and Schubert 1974). The purpose of this paper is to investigate the GCAPE of conditionally unstable soundings and its possible relevance to the problem of cumulus parameterization.

2. The GCAPE of GATE soundings

We have computed the GCAPE of GATE soundings, as analyzed by Thompson et al. (1979), using a modified version of the parcel-moving (PM) algorithm discussed by L79. The data used here, kindly provided by R. Reed, consist of a single sounding for each of 157 GATE Phase III observation times. The thermodynamic formulas used are given in appendix A, while the PM algorithm itself is described in appendix B. We also tested a "brute force" method, which checks all possible permutations of the parcels and selects the permutation for which H is minimized. This approach is feasible only when the number of parcels under consideration is less than about 10. In order to apply the PM algorithm, each sounding is divided into N parcels; initially $N = 9$ was used.

To our initial surprise, all of the GATE soundings tested were found to have zero GCAPE, i.e., the given states were the same as the reference states. This result was obtained with both the PM and brute force algorithms. An example of such a sounding, for 1800 UTC 30 August, is given in Fig. 1. It is clear that conditional instability exists, so that GCAPE *must* be present. At first, a programming error was suspected.

After further investigation, we determined that the reason that many of the GATE soundings were found to have no GCAPE at all is simple enough: the parcels that were being moved around, which ranged in size from about 30 mb to about 100 mb, were too massive. The problem with such massive parcels can be understood through the following argument. In convectively active situations, the cumulus mass flux is typically on

TABLE 1. Results of the parcel-moving method for GATE observation time 71. Here RH is the relative humidity. The GCAPE is 11.12 J kg^{-1}.

	Given sounding						Reference sounding							
Level	p (mb)	T (K)	$\bar{w}$ (g kg^{-1})	RH (%)	θ_v (K)	p_{sat} (mb)	p (mb)	T (K)	$\bar{w}$ (g kg^{-1})	RH (%)	θ_v (K)	$\bar{w} - w$ (g kg^{-1})	$T_R - T$ (K)	$\bar{w}_R - \bar{w}$ (g kg^{-1})
1	112.5	197.3	0.008	67.7	368.28	106.78	112.5	197.3	0.008	67.7	368.28	.000	0.00	0.00
2	137.5	201.6	0.008	41.3	355.24	121.94	137.5	201.6	0.008	41.3	355.24	.000	0.00	0.00
3	162.5	207.3	0.014	40.1	348.30	142.87	162.5	210.8	17.05	30 936.9	348.32	16.993	13.53	17.03
4	187.5	213.3	0.028	42.5	344.13	165.41	187.5	215.9	0.014	15.3	348.30	.000	2.59	−0.01
5	212.5	219.7	0.051	40.7	341.98	185.30	212.5	221.1	0.028	18.8	344.13	.000	1.38	−0.02
6	237.5	225.9	0.096	41.9	340.56	206.98	237.5	226.8	0.051	20.3	341.98	.000	0.94	−0.04
7	262.5	231.7	0.130	33.7	339.44	220.03	262.5	232.4	0.096	22.9	340.56	.000	0.77	−0.03
8	287.5	237.2	0.223	36.0	338.63	242.18	287.5	237.8	0.130	19.8	339.44	.000	0.58	−0.09
9	312.5	242.1	0.285	30.9	337.56	255.37	312.5	242.9	0.223	22.5	338.63	.000	0.78	−0.06
10	337.5	246.4	0.335	26.4	336.06	267.24	337.5	247.5	0.285	20.2	337.56	.000	1.11	−0.05
11	362.5	250.3	0.422	25.1	334.52	283.15	362.5	251.5	0.335	18.0	336.06	.000	1.16	−0.09
12	387.5	254.0	0.617	28.5	333.03	308.02	387.5	255.1	0.422	17.7	334.52	.000	1.16	−0.20
13	412.5	257.3	0.931	34.4	331.54	337.74	412.5	258.5	0.617	20.6	333.03	.000	1.20	−0.31
14	437.5	260.4	1.338	40.8	329.97	368.39	437.5	261.7	0.931	25.5	331.54	.000	1.30	−0.41
15	462.5	262.9	1.972	51.8	328.08	406.46	462.5	264.5	1.338	30.9	329.97	.000	1.60	−0.63
16	487.5	265.0	2.946	69.1	325.95	452.63	487.5	266.9	1.972	40.0	328.08	.000	1.88	−0.97
17	512.5	267.1	3.774	79.6	323.91	489.23	512.5	268.9	2.946	54.2	325.95	.000	1.80	−0.83
18	537.5	269.0	4.578	87.4	322.01	522.70	537.5	270.7	3.774	63.3	323.91	.000	1.71	−0.80
19	562.5	270.7	5.225	91.5	320.04	552.17	562.5	272.5	4.578	70.3	322.01	.000	1.76	−0.65
20	587.5	272.5	5.806	93.0	318.30	578.53	587.5	274.1	5.225	74.5	320.04	.000	1.58	−0.58
21	612.5	274.6	6.329	90.9	317.01	600.19	612.5	275.8	5.806	76.5	318.30	.000	1.20	−0.52
22	637.5	276.6	7.209	93.2	315.88	627.95	637.5	277.8	6.329	75.5	317.01	.000	1.13	−0.88
23	662.5	278.5	7.584	89.4	314.59	646.64	662.5	279.7	7.209	78.2	315.88	.000	1.20	−0.38
24	687.5	280.3	8.204	88.3	313.45	669.05	687.5	281.4	7.584	75.6	314.59	.000	1.12	−0.62
25	712.5	282.0	8.766	87.0	312.27	690.85	712.5	283.2	8.204	75.2	313.45	.000	1.16	−0.56
26	737.5	283.6	8.719	80.3	310.97	702.38	737.5	284.8	8.766	74.5	312.27	.000	1.18	0.05
27	762.5	285.2	8.730	74.7	309.75	714.59	762.5	286.3	8.719	69.2	310.97	.000	1.13	−0.01
28	787.5	286.5	8.456	68.7	308.23	724.22	787.5	287.8	8.730	64.8	309.75	.000	1.36	0.27
29	812.5	287.5	9.172	71.9	306.71	754.47	812.5	289.0	8.456	59.9	308.23	.000	1.54	−0.72
30	837.5	288.6	10.67	80.4	305.48	796.96	837.5	290.0	9.172	63.0	306.71	.000	1.41	−1.50
31	862.5	289.8	11.51	82.8	304.32	825.99	862.5	291.0	10.67	70.7	305.48	.000	1.25	−0.85
32	887.5	291.2	12.63	85.4	303.52	855.73	887.5	292.1	11.51	73.2	304.32	.000	0.96	−1.12
33	912.5	292.6	13.45	85.2	302.78	879.12	912.5	293.5	12.63	75.8	303.52	.000	0.85	−0.82
34	937.5	294.1	14.73	87.4	302.19	908.45	937.5	294.9	13.45	75.9	302.78	.000	0.80	−1.28
35	962.5	295.7	16.60	91.4	301.92	942.28	962.5	296.3	14.73	78.2	302.19	.000	0.58	−1.88
36	987.5	297.5	16.82	85.2	301.55	950.83	987.5	297.9	16.60	82.1	301.92	.000	0.41	−0.02
37	1006.2	298.8	17.05	81.1	301.33	957.37	1006.2	299.1	16.82	78.8	301.55	.000	0.25	−0.23

the order of 200–300 mb per day (e.g., Yanai et al. 1973; Cheng 1989). This means that 200–300 mb per day of boundary-layer mass is carried upward in cumulus towers, while the free-atmospheric environment sinks at a comparable rate. Experiments with numerical cloud models show, however, that the conditional instability present in real soundings can be released by convection within a couple of hours (e.g., Soong and Tao 1980; Dudhia and Moncrieff 1987; Krueger 1988). This means that, in the absence of a forcing mechanism to replenish the instability, only on the order of 20 mb ($1/12$ of 240 mb) of mass can rise to the tropopause before the GCAPE is exhausted. It follows that, in order to obtain an accurate estimate of the GCAPE, the 800-mb–deep troposphere must be divided into about 40 parcels, each 20 mb deep.

We have applied the PM algorithm described in appendix B to all 157 observation times of GATE Phase III (Thompson et al. 1979). With $N = 9$, no GCAPE is detected in any of the soundings. Table 1 shows an example of how parcels are rearranged from the given state to the reference state for observation time 71, with $N = 37$. In this case, the parcel nearest the surface in the given state rises to 162 mb in the reference state, and all of the intervening parcels are shifted down by one level. Since the lifted parcel conserves its total mixing ratio (we allow no precipitation), its liquid water content in the reference state is extremely large. Below the 162-mb level, the troposphere is warmed and dried by the "compensating subsidence."

Figure 2 shows the time variation of the GCAPE determined with 37 and 100 parcels; also shown, for comparison, is the time variation of the cloud work function for the case of no entrainment (Arakawa and Schubert 1974). Increasing the number of parcels from 37 to 100 does not make much difference in the GCAPE. There is a strong positive correlation between the GCAPE and the cloud work function. Note, however, that the numerical values of these quantities are radically different. The reason is, quite simply, that their physical meanings are different. The cloud work function represents the kinetic energy per unit mass that can be realized by a parcel rising in a convective updraft. It is apparent from (1.1) that, in contrast, the GCAPE represents the kinetic energy per unit mass that can be realized by all of the air in the column, including rapid convective updrafts and downdrafts, their relatively lethargic large-scale environment, and the horizontal flows that connect these vertical currents together. This explains why the numerical values of the GCAPE are considerably smaller than those of the cloud work function.

Figure 3 shows the time variations of $T_R - T$ and $\bar{w}_R - \bar{w}$, which are, respectively, the departure of the reference state temperature from that of the given state and the departure of the reference state total mixing ratio (vapor plus liquid) from that of the given state. Significant fluctuations occur, and these are correlated in a straightforward way with the fluctuations of the GCAPE shown in Fig. 2. The "black spots" seen in the plots, mainly in the upper troposphere, show the locations, in the reference state, of parcels that originate at low levels in the given state (see Table 1).

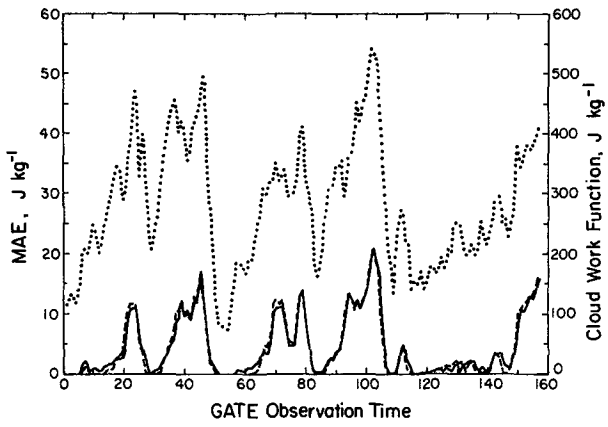

FIG. 2. The time variation of the GCAPE as determined by the PM algorithm with 37 and 100 parcels. Also shown is the time variation of the cloud work function for the case of no entrainment. The cloud work function was determined using nine equally spaced levels; the updrafts were assumed to originate at the lowest level.

Figure 4 shows the time averages of $T_R(p)$, $T(p)$, $\bar{w}_R(p)$, and $\bar{w}(p)$ over the 157 GATE observation times. Not surprisingly, the average reference sounding is systematically warmer and drier than the average given sounding, except in the upper troposphere where the lifted parcels are of course much wetter than those they displace.

Figure 5 shows the departures of $T_R(p)$ and $T(p)$ from their respective time averages, as well as the departures of $\bar{w}_R(p)$ and $\bar{w}(p)$ from their respective time averages. It is clear that *at each pressure level the reference state and the given state tend to vary together.*

Figure 6 makes this point more explicitly by showing the correlations of $T_R(p)$ with $T(p)$ and of $\bar{w}_R(p)$ with $\bar{w}(p)$ as functions of pressure. To compute these correlations, we included, at each level, all of the observation times for which the GCAPE was found to be positive and the transition from the given state to the reference state involved parcel exchanges at levels up to or beyond the level in question. The figure shows that $T_R(p)$ and $T(p)$ are well correlated below about 700 mb and are moderately well correlated up to 200 mb. Similarly, $\bar{w}_R(p)$ and $\bar{w}(p)$ are very well correlated up to 300 mb, except near 950 mb, 700 mb, and 450 mb. Large positive correlations indicate that changes in the observed state are systematically "tracking" those of the reference state. As mentioned above, the correlations shown in Fig. 6 are relatively weak near 950 mb, 700 mb, and 450 mb. The 950-mb level is within the boundary layer, and the 700-mb and 450-mb levels are where lifted parcels frequently come to rest in the reference state, as shown in Fig. 3.

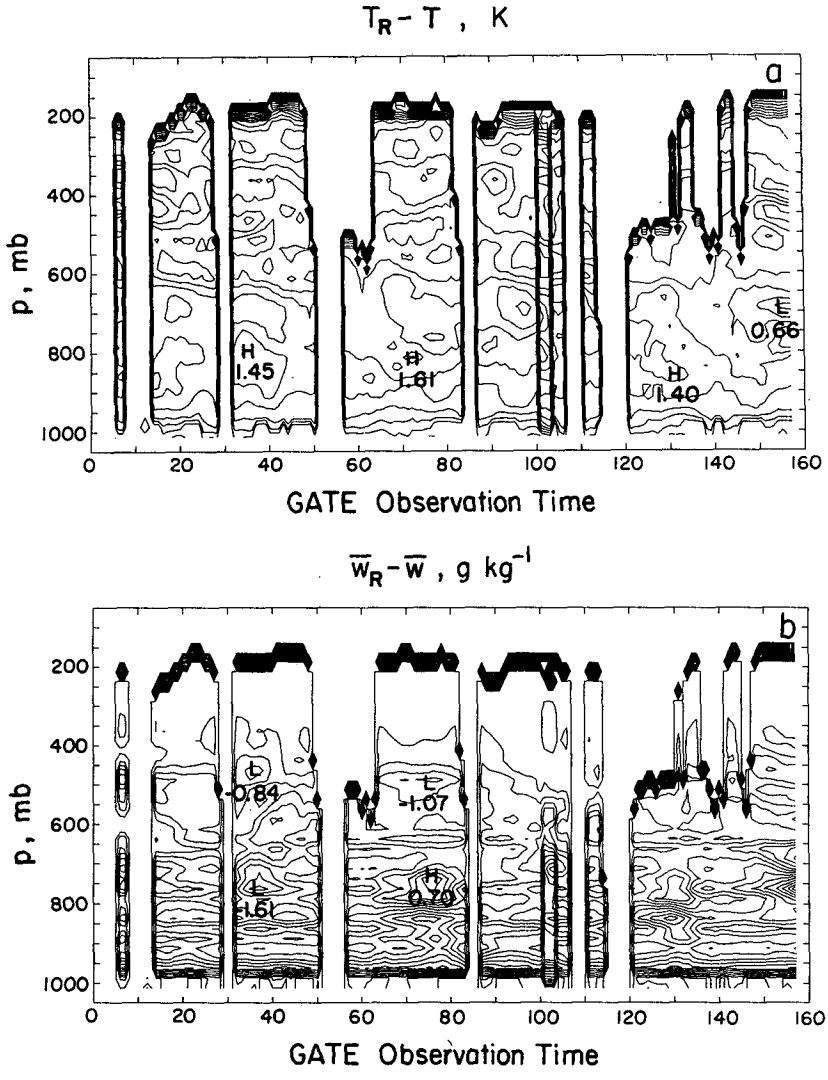

FIG. 3. The time variations of $T_R - T$ and $\bar{w}_R - \bar{w}$, which are, respectively, the departure of the reference state temperature from that of the given state and the departure of the reference state total mixing from that of the given state. The contour interval is 0.25 K for $T_R - T$ and 0.1 g kg^{-1} for $\bar{w}_R - \bar{w}$.

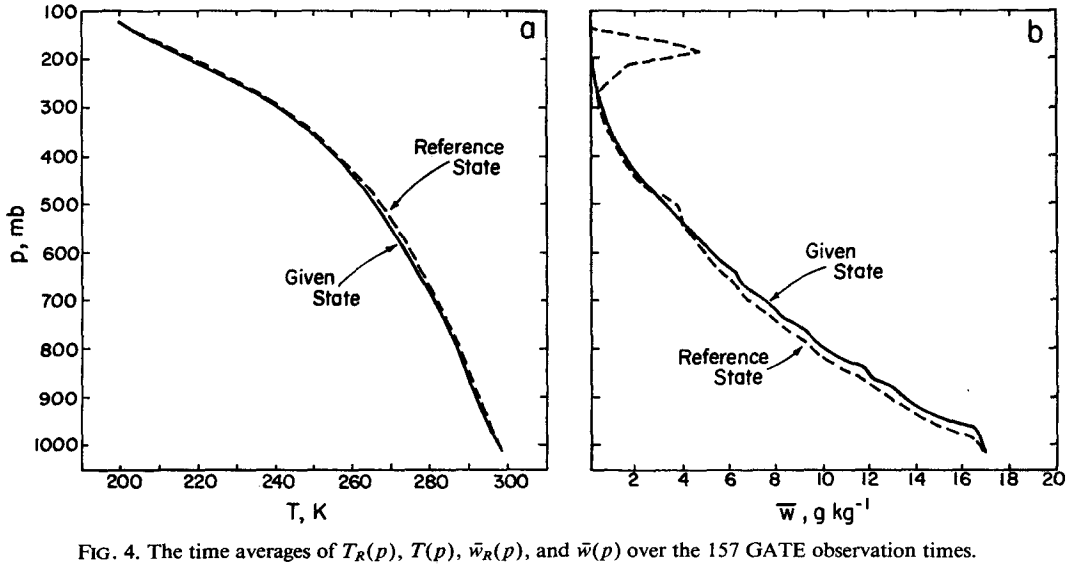

FIG. 4. The time averages of $T_R(p)$, $T(p)$, $\bar{w}_R(p)$, and $\bar{w}(p)$ over the 157 GATE observation times.

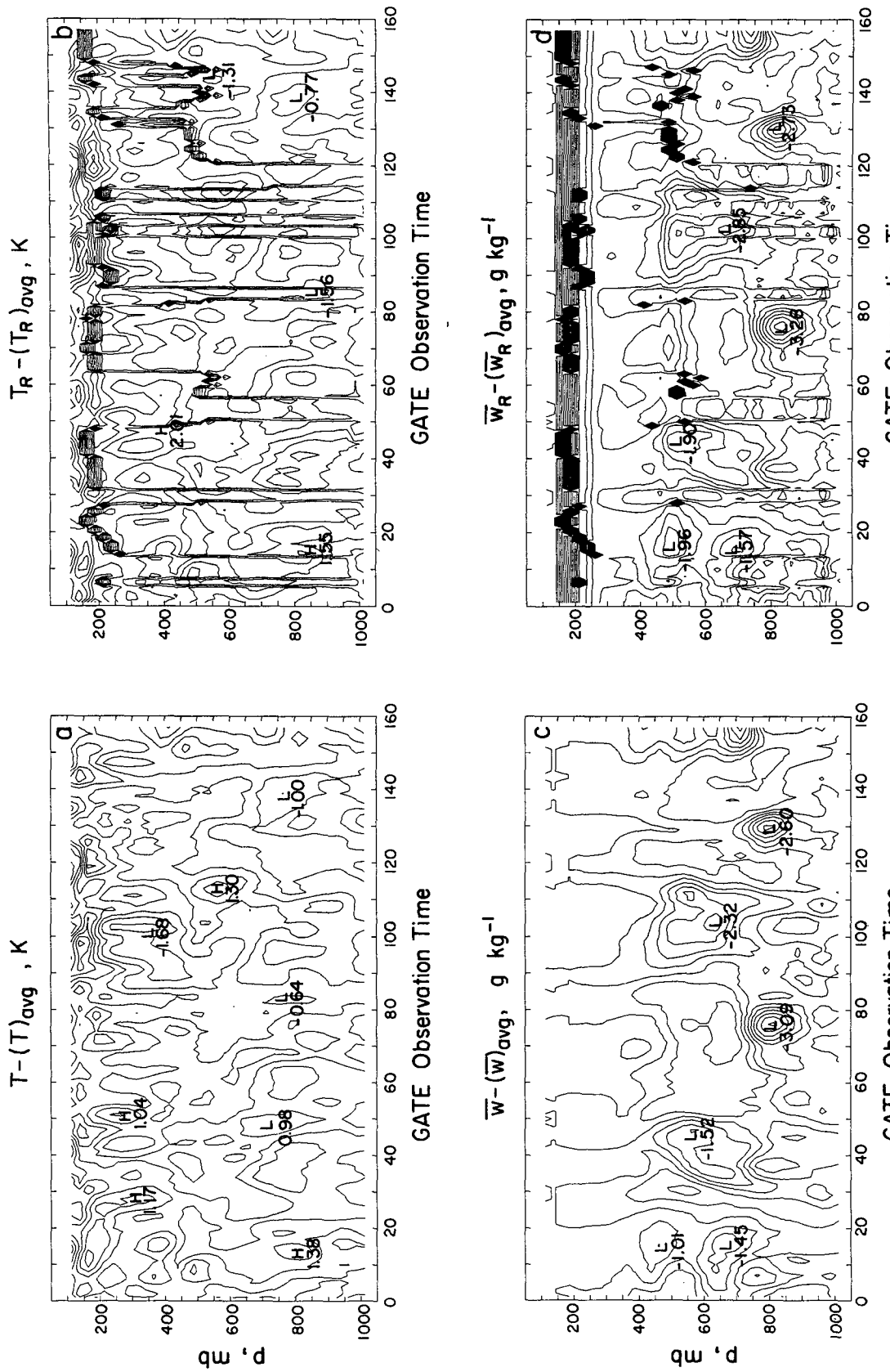

FIG. 5. The departures of $T_R(p)$ and $T(p)$ from their respective time averages, and also the departures of $\bar{w}_R(p)$ and $\bar{w}(p)$ from their respective time averages. For the temperatures, the contour interval is 0.5 K, and for the mixing ratios it is 0.1 g kg^{-1}.

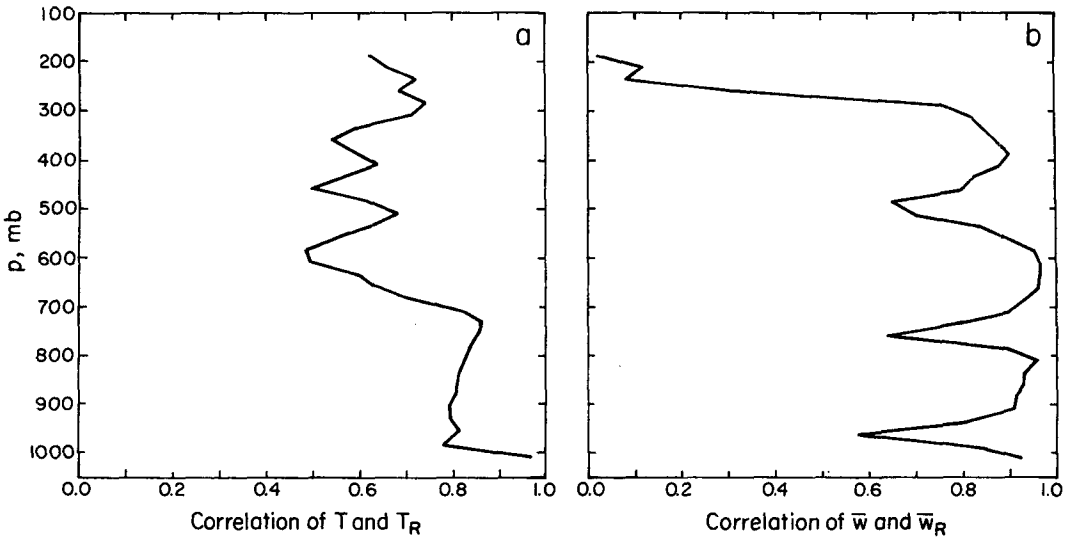

FIG. 6. The temporal correlations of $T_R(p)$ with $T(p)$, and of $\bar{w}_R(p)$ with $\bar{w}(p)$, as functions of pressure.

3. A mass flux algorithm to determine the GCAPE

It is somewhat impractical to divide each sounding into scores or hundreds of parcels; an alternative approach is as follows. We divide the given sounding into N layers, where N is a manageable number of order 10. Let the mass of layer i be denoted by m_i. Imagine that a system of "pipes" is set up, connecting each layer of the sounding with every other layer. Each pipe allows mass to be transferred adiabatically and reversibly in a single direction. Let the amount of mass transferred from layer i to layer j be $M_{i,j}$. We will use a prime to denote a variable in the reference state. For an intensive variable A that is conserved under adiabatic reversible processes, we can write

$$m_i'A_i' = m_iA_i + \sum_{j=1}^{N} M_{j,i}\hat{A}_j - \sum_{j=1}^{N} M_{i,j}\hat{A}_i, \quad (3.1)$$

where $\hat{A}$ denotes a "source" value of A that must be specified. This source value represents a typical value of A in the layer from which mass is removed. When mass flows from layer j to layer i, the source value should be characteristic of layer j, and vice versa. For this reason, we must require that $M_{i,j} \geqslant 0$.

Three obvious possible choices of $\hat{A}$ are:

$$\hat{A}_j = A_j, \quad (3.2a)$$

$$\hat{A}_j = A_j', \quad (3.2b)$$

$$\hat{A}_j = (A_j + A_j')/2. \quad (3.2c)$$

We shall refer to these as the "forward," "backward," and "trapezoidal" schemes, respectively. The trapezoidal scheme has the advantage that it is reversible, which is in accord with our wish to consider reversible adiabatic processes. It also has other advantages as described below. We use the trapezoidal scheme in this paper. Putting $A \equiv 1$ in (3.1) gives a mass conservation equation:

$$m_i' = m_i + \sum_{j=1}^{N} (M_{j,i} - M_{i,j}). \quad (3.3)$$

We allow only "eddy" mass exchange, so that

$$m_i' = m_i, \quad (3.4)$$

$$\sum_{j=1}^{N} (M_{j,i} - M_{i,j}) = 0. \quad (3.5)$$

Of course, the diagonal elements $M_{i,i}$ can be set to zero. Using (3.3)–(3.5), (3.1) can be rewritten as

$$\left(m_i + \sum_{j=1}^{N} \frac{1}{2} M_{j,i}\right)(A_i' - A_i) - \sum_{j=1}^{N} \frac{1}{2} M_{j,i}(A_j' - A_j) = \sum_{j=1}^{N} M_{j,i}(A_j - A_i). \quad (3.6)$$

These equations can be used to evaluate the GCAPE of conditionally unstable soundings. If a set of $M_{i,j}$ is specified, (3.6) can be applied to determine the changes in the entropy and total mixing ratio of the air. The total enthalpy of the new state can then be evaluated and compared with that of the given state. *We seek the matrix $M_{i,j}$ such that the total enthalpy of the final state is minimized, subject to the constraint (3.5).* Of course, we must also restrict ourselves to nonnegative M's.

With this mass flux method, as with the parcel-moving method, a conditionally unstable given state corresponds to a reference state in which some portion of the air must be saturated. As a result, the amount of

mass lifted from lower levels to upper levels may have to attain a finite minimum value before any decrease in the total enthalpy occurs. It should also be noted that (3.6) only determines the *average* entropy and total mixing ratio of the adjusted state; the adjusted enthalpy has to be based on these average values.

As an example, consider the simple case $N = 2$. Then (3.5) implies that

$$M_{1,2} = M_{2,1} = M. \tag{3.7}$$

After some manipulation, we find from (3.6) that

$$A_1' - A_1 = \frac{m_2 M(A_2 - A_1)}{m_1 m_2 + \frac{1}{2} M(m_1 + m_2)}, \tag{3.8}$$

$$A_2' - A_2 = \frac{-m_1 M(A_2 - A_1)}{m_1 m_2 + \frac{1}{2} M(m_1 + m_2)}. \tag{3.9}$$

For $M \to \infty$, and if $m_1 = m_2$, (3.8) and (3.9) imply that the parcels exchange places: parcel number 1 takes property A_2, and vice versa. The trapezoidal scheme thus gives us a parcel swapper in the limit of large M. This is an attractive property of the scheme.

We have applied these equations to the idealized two-level "sounding" given in Table 2; θ is the potential temperature, θ_e is equivalent potential temperature, and θ_{es} is saturation equivalent potential temperature. The two layers are assumed to be of equal thickness, with surface pressure 1000 mb and top pressure 100 mb. Both levels are nearly saturated. The relative humidity at 775 mb is so high that even slight lifting is sufficient to produce condensation. Since the θ_e of the lower layer exceeds the θ_{es} of the upper layer, the sounding is conditionally unstable. Following L79, we assume that entropy and total mixing ratio are conserved. We tried various values of M/m_2, increasing from zero by steps of 0.01. The results are shown in Fig. 7. The upper level becomes saturated with even a one percent injection of air from the lower level. A minimum of the total enthalpy occurs for $M/m_2 = 0.11$; this corresponds to the reference state. The GCAPE per unit mass is 13.1 J kg^{-1}. In the limit $M/m_2 \to \infty$, the change in H approaches 1397 J kg^{-1}. Clearly, for this particular case the behavior of the algorithm as $M \to \infty$ is irrelevant.

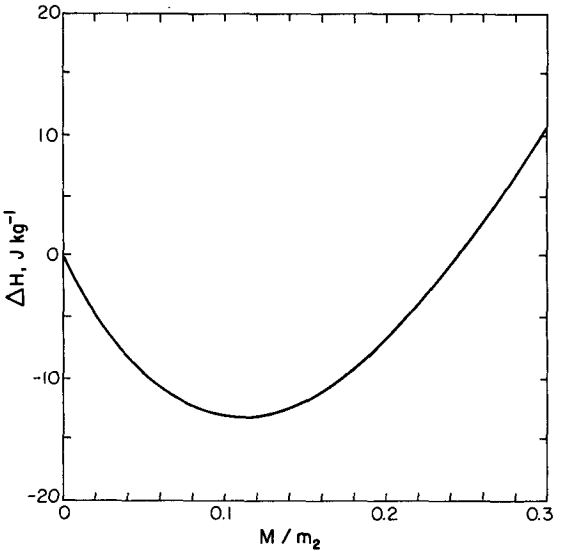

FIG. 7. Departure of the total enthalpy from that of the given state, plotted as a function of M/m_2, for the two-level "sounding" given in Table 2. Here M is the amount of mass exchanged between the layers, and m_2 is the mass of the lower layer.

4. Penetrators

For $N > 2$, we need a way to ensure that (3.5) is automatically satisfied. This is done by introducing "penetrators." A penetrator $P_{i,j}$ consists of a mass flux that penetrates from layer i to layer j, with a compensating, *nonpenetrative, level-by-level return flow*. Each penetrator satisfies (3.5), so any superposition of penetrators also satisfies (3.5). By analogy with (3.1), the change in A_i due to an ensemble of penetrators is given by

$$\begin{aligned} m_i' A_i' - m_i A_i = & \sum_{j=1}^{N} P_{j,i}(\hat{A}_j - \hat{A}_i) \\ & - \sum_{j=1}^{N} P_{i,j}\hat{A}_i + \sum_{j<i} P_{i,j}\hat{A}_{i-1} + \sum_{j>i} P_{i,j}\hat{A}_{i+1} \\ & + \sum_{j<i} \sum_{l>i} P_{j,l}(\hat{A}_{i+1} - \hat{A}_i) + \sum_{j>i} \sum_{l<i} P_{j,l}(\hat{A}_{i-1} - \hat{A}_i). \end{aligned} \tag{4.1}$$

On the right-hand side of (4.1), the terms on the first line represent the effects of "incoming" penetrators that terminate at level i, those on the second line represent the effects of "outgoing" penetrators that originate at level i, and the terms on the third line represent the effects of penetrators that are "just passing through" level i. Putting $A \equiv 1$, and using

$$P_{i,i} = 0 \tag{4.2}$$

for all i, we find that (4.1) reduces to

$$m_i' - m_i = 0; \tag{4.3}$$

this is identical to (3.4), and it follows immediately that (3.5) is automatically satisfied by any combination of penetrators as intended.

TABLE 2. A hypothetical two-level sounding used to generate the results shown in Fig. 7.

p (mb)	T (K)	θ (K)	q (g kg^{-1})	θ_e (K)	θ_{es} (K)
325	250	344.78	1.78	350.86	351.04
775	290	311.93	15.70	354.71	354.89

We assume that any combination of mass fluxes satisfying (3.5) is equivalent to a suitably chosen combination of penetrators. After some algebraic manipulation, (4.1) can be rewritten as

$$m_i(A_i' - A_i) = \sum_{|j-i|>1} P_{j,i}(\hat{A}_j - \hat{A}_i) + (\hat{A}_{i-1} - \hat{A}_i)(Q_{i,i-1} + \sum_{j<i-1} P_{i,j} + \sum_{j>i} \sum_{l<i} P_{j,l}) + (\hat{A}_{i+1} - \hat{A}_i)(Q_{i,i+1} + \sum_{j>i+1} P_{i,j} + \sum_{j<1} \sum_{l>i} P_{j,l}), \quad (4.4)$$

where

$$Q_{i,i-1} \equiv P_{i,i-1} + P_{i-1,i}. \quad (4.5)$$

Notice that $P_{i,i-1}$ and $P_{i,i+1}$ do not appear explicitly in (4.4), although they do appear implicitly through $Q_{i,i-1}$ and $Q_{i,i+1}$. The interpretation is straightforward. A penetrator that joins two neighboring layers does not really penetrate at all. As a result, the injection of air from i to $i + 1$ with the accompanying return flow from $i + 1$ to i has exactly the same effect as injection from $i + 1$ to i with a return flow from i to $i + 1$. This means that $P_{i+1,i}$ and $P_{i,i+1}$ are redundant; they do the same thing. That is why only their sum, $Q_{i,i+1}$, appears in (4.4).

To determine the reference state and the GCAPE, we must find the values of the P and Q such that the total enthalpy of the adjusted state is minimized. These solutions are subject to the requirement that the P and Q must be nonnegative, since their source regions have been specified. For an N-layer sounding, we can define N^2 different values of P. Not all of these are meaningful, however. As indicated in (4.2), the diagonal elements of the P matrix can be set to zero, since they have no effect on the sounding. In addition, the redundancy of the neighboring-layer P, discussed above, allows us to replace $2(N - 1)$ of the P by $(N - 1)Q$, effectively reducing the number of unknowns by $N - 1$. The actual number of unknowns is then $N^2 - N - (N - 1) = (N - 1)^2$. In general, there are $(N - 1)Q$ and $(N - 2)(N - 1)P$. Table 3 shows how the numbers of the various unknowns change as N changes. Given the results of section 2, we can anticipate that, in most cases of practical interest, many of these unknowns will turn out to be zero. Unfortunately, there is no obvious way to know in advance which ones these will be.

TABLE 3. The numbers of P and Q and the total number of unknowns as a function of the number of model layers.

Number of layers	Number of P	Number of Q	Total number of unknowns
2	0	1	1
3	2	2	4
4	6	3	9
5	12	4	16
6	20	5	25
7	30	6	36
8	42	7	49
9	56	8	64
10	72	9	81

5. Application of penetrators to the GATE data

For selected GATE observation times, and allowing only 9 layers, we have considered each possible P and each possible Q, one at a time, and computed the greatest possible reduction in total enthalpy and the corresponding fraction of mass transported out of the layer from which the penetrator originates. For GATE observation time 102, Fig. 8 illustrates the change in the total enthalpy as a function of $P_{i,j}/m_i$ for four different choices of i and j. The results are plotted for $0 \leq P_{i,j}/m_i \leq 1$, although in principle arbitrarily large positive values could be considered. In the first case, the enthalpy increases monotonically, so that no GCAPE can be realized. In the second case, a single well-defined minimum of the total enthalpy occurs for $P_{i,j}/m_i = 0.55$; this is similar to Fig. 7. In the third case, the enthalpy decreases monotonically out to $P_{i,j}/m_i = 1.0$, suggesting that ΔH is minimized in the limit as $P_{i,j}/m_i \to \infty$. In the fourth case, a broad, flat minimum of the total enthalpy occurs for $0.2 < P_{i,j}/m_i < 0.6$.

These four cases illustrate all of the behaviors that we have found in the GATE data. Cases for which multiple, distinct enthalpy minima occur for distinct values of the penetrator mass flux were not encountered. We have not proven that such cases cannot occur, however.

Table 4 shows the maximum total enthalpy reduction that can be produced by each penetrator for several GATE observation times, and Table 5 shows the corresponding values of $P_{i,j}/m_i$. These results are for $N = 9$. Recall that the parcel-moving algorithm did not detect any GCAPE with $N = 9$. Clearly the penetrator algorithm has succeeded in detecting the GCAPE that is present in the soundings. As discussed earlier, zeroes are guaranteed to occur, in both tables, along the diagonals that run from top left to bottom right, since these trivial "penetrators" have no effect on the soundings. Entries below the diagonals represent penetrators

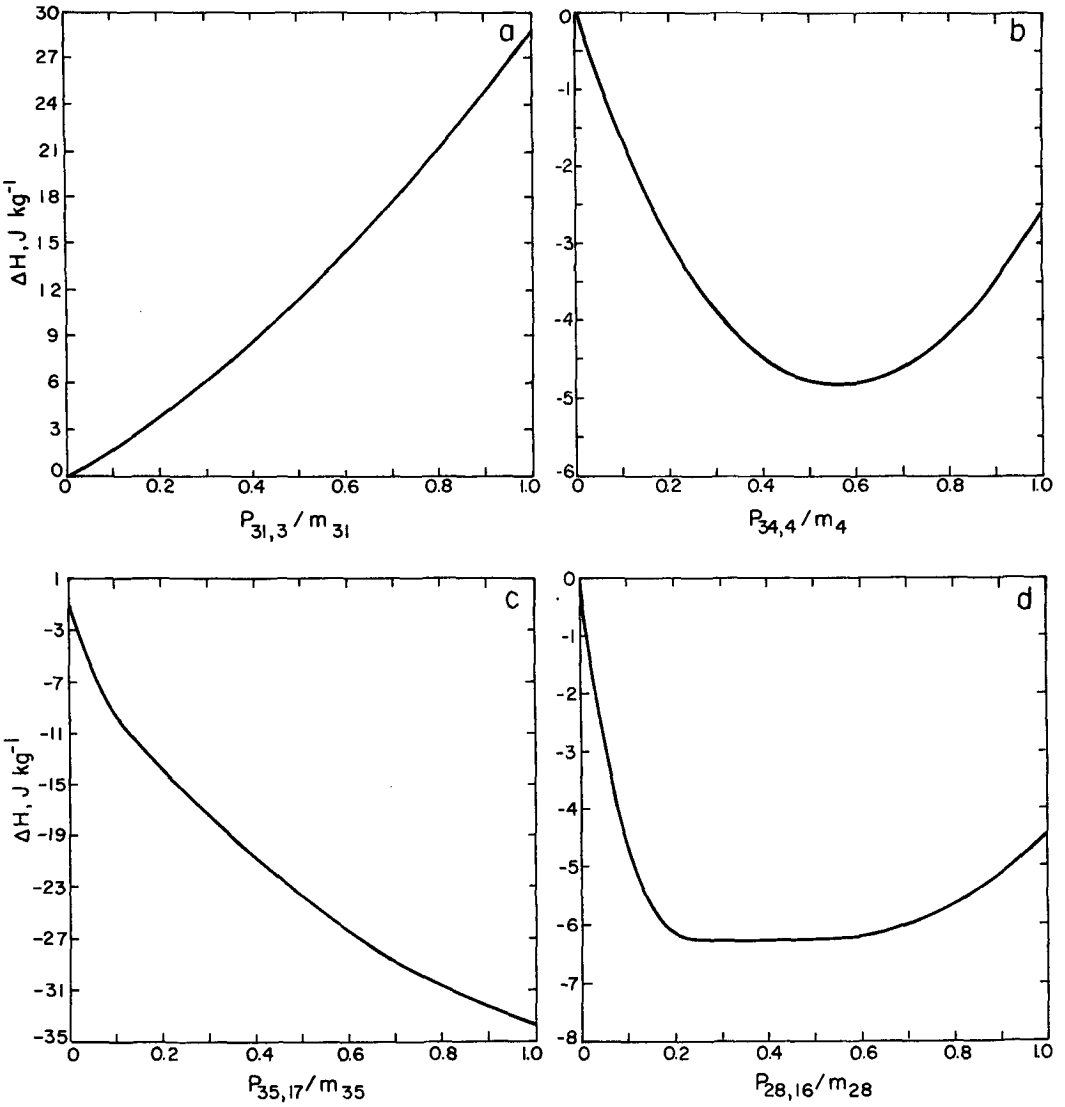

FIG. 8. The change in the total enthalpy as a function of $P_{i,j}/m_i$, for: (a) $i = 31$ and $j = 3$ (penetrator originating at 862 mb and terminating at 162 mb); (b) $i = 34$ and $j = 4$ (penetrator originating at 937 mb and terminating at 187 mb); (c) $i = 35$ and $j = 17$ (penetrator originating at 962 mb and terminating at 512 mb); and (d) $i = 28$ and $j = 16$ (penetrator originating at 787 mb and terminating at 487 mb). The GATE observation time is 102.

that penetrate upward, with a compensating downward layer-by-layer return flow; and entries above the diagonal represent penetrators that penetrate downward, with a compensating upward layer-by-layer return flow. The entries nearest the diagonals represent Q, and (4.5) guarantees that they are symmetric, i.e., $Q_{i,i-1} = Q_{i-1,i}$. We naturally expect upward penetrators to dominate, and they do, with the largest number of nonzero entries and the largest enthalpy reductions, particularly for penetrators originating near the lower boundary and penetrating to the upper troposphere.

Surprisingly, however, our results show that it is possible for downward penetrators to release GCAPE in some cases. For example, at GATE observation time 45, a penetrator originating at 447 mb can release GCAPE by penetrating downward to 782 mb or below. In such cases, the compensating layer-by-layer upward motion produces condensation, and this accounts for the release of available energy. Although it may well be dynamically impossible for such penetrators to develop, this issue deserves further study.

How can we determine the set of P and Q that is required to reach the reference state for the case of arbitrary N? For $N = 2$, discussed in section 3, we searched a one-dimensional space by brute force to find the value of the single unknown, which we now recognize as a Q. A glance at Table 3 shows that this approach quickly becomes impractical for arbitrary N.

As an alternative, we could use a numerical method to determine the partial derivative H with respect to

TABLE 4. The maximum enthalpy reduction produced by each penetrator for several GATE observation times using nine layers. Zeroes are omitted from the tables. The row indicates the pressure from which the penetrator originates, while the column indicates the pressure to which the penetrator penetrates.

	112.5	224.2	335.9	447.6	559.3	671.0	782.7	894.4	1006.1
				GATE observation time 4					
112.5									
224.2									
335.9									
447.6					1.03				
559.3				1.03					0.06
671.0							7.36	5.59	9.23
782.7				0.36		7.36		0.32	4.48
894.4				1.14		6.80	0.32		7.49
1006.1		1.28	3.78	8.80	7.61	18.81	7.61	7.49	
				GATE obseration time 45					
112.5									
224.2									
335.9									
447.6							0.68	5.23	4.26
559.3						3.77	9.74	21.59	19.73
671.0				0.29	3.77		9.05	24.39	23.87
782.7				7.81	15.76	9.05		12.58	13.17
894.4		0.01	4.17	28.20	38.70	27.48	12.58		2.29
1006.1		20.61	33.23	61.30	65.22	45.16	19.62	2.29	
				GATE observation time 69					
112.5									
224.2									
335.9					4.30	0.70			0.04
447.6					14.36	5.53	0.03	1.67	2.35
559.3			6.33	14.36				0.02	0.68
671.0			7.66	12.06				0.06	1.62
782.7			2.36	2.40				7.98	17.33
894.4			6.36	7.36		0.01	7.98		13.01
1006.1		25.26	33.42	29.42	13.91	13.95	27.15	13.01	
				GATE observation time 85					
112.5									
224.2									
335.9									
447.6									
559.3									
671.0								0.25	2.19
782.7								3.16	8.54
894.4						0.40	3.16		6.74
1006.1		1.60	5.07	5.47	6.68	9.84	12.75	6.74	
				GATE observation time 102					
112.5									
224.2									
335.9									
447.6							2.76	8.10	5.37
559.3						1.71	19.68	30.72	24.94
671.0					1.71		24.86	36.93	31.94
782.7				1	25.46	24.86		9.15	8.81
894.4		0.72	6.93	29.29	45.89	37.82	9.15		2.20
1006.1		28.40	0.80	63.85	72.64	52.96	15.21	2.20	

each of the P and Q. The results could be arranged as a matrix. We could then try a linearization approximation in which this matrix is used to find the values of the P and Q that minimize H. Unfortunately, this approach fails, for two reasons. First, it cannot guarantee that the P and Q are nonnegative. Second, as is

TABLE 5. The values of $P_{i,j}/m_i$ associated with the maximum enthalpy reduction by each penetrator for several GATE observation times using nine layers. Zeroes are omitted from the tables. The row indicates the pressure from which the penetrator originates, while the column indicates the pressure to which the penetrator penetrates.

	112.5	224.2	335.9	447.6	559.3	671.0	782.7	894.4	1006.1
				GATE observation time 4					
112.5									
224.2									
335.9									
447.6					0.07				
559.3				0.07					0.01
671.0							0.24	0.17	0.19
782.7				0.02		0.24		0.06	0.18
894.4				0.04		0.17	0.06		0.36
1006.1		0.08	0.14	0.21	0.30	0.39	0.28	0.36	
				GATE observation time 45					
112.5									
224.2									
335.9									
447.6							0.04	0.11	0.10
559.3						0.15	0.20	0.27	0.26
671.0				0.02	0.15		0.30	0.37	0.35
782.7				0.11	0.22	0.30		0.36	0.32
894.4		0.01	0.18	0.44	0.56	0.56	0.36		0.22
1006.1		0.34	0.51	0.73	0.84	0.81	0.55	0.22	
				GATE observation time 69					
112.5									
224.2									
335.9					0.10	0.04			0.01
447.6					0.23	0.13	0.01	0.06	0.07
559.3			0.08	0.23				0.01	0.04
671.0			0.07	0.16				0.02	0.09
782.7			0.03	0.06				0.27	0.36
894.4			0.05	0.09		0.01	0.27		0.55
1006.1		0.34	0.41	0.39	0.37	0.43	0.55	0.55	
				GATE observation time 85					
112.5									
224.2									
335.9									
447.6									
559.3									
671.0								0.04	0.10
782.7								0.19	0.25
894.4						0.04	0.19		0.35
1006.1		0.09	0.16	0.20	0.26	0.36	0.39	0.35	
				GATE observation time 102					
112.5									
224.2									
335.9									
447.6							0.09	0.15	0.12
559.3						0.10	0.29	0.33	0.30
671.0					0.10		0.45	0.43	0.39
782.7				0.12	0.28	0.45		0.31	0.26
894.4		0.06	0.26	0.47	0.60	0.55	0.31		0.23
1006.1		0.43	0.56	0.75	0.86	0.80	0.46	0.23	

clear from Figs. 7 and 8, H varies nonlinearly with the P and Q. This nonlinearity arises from the nonlinear dependence of the enthalpy of saturated air on the entropy and total mixing ratio. The nonlinearity is actually critical for the existence of an isolated *minimum* value of H for finite positive values of the P and Q.

To see this, consider the *dry* statically unstable case with $N = 2$, as discussed in the Introduction. If the trapezoidal algorithm is used, we find that there is no minimum of H for finite Q. Instead, H decreases monotonically as Q increases and is minimized when $Q \to \infty$, i.e., when the parcels are swapped.

The nonlinearity also rules out the use of linear programming methods, which, if they were applicable, could ensure nonnegativity of the P and Q. It appears that we must employ nonlinear programming, which is relatively unknown territory with few strong theorems. This problem is left to the future.

6. Summary and concluding discussion

We have demonstrated that the concept of moist available energy, as formulated by Lorenz (1978, 1979), can be used to define a generalized convective available kinetic energy. An advantage of this GCAPE is that it can be determined without arbitrary assumptions about the level of origination of the convective updrafts. It can also include, without modification, the effects of evaporatively cooled convective downdrafts originating from elevated cloud layers, as well as the energetic consequences of compensating vertical motions in the environment of the concentrated vertical currents.

Using GATE data, we have demonstrated that the GCAPE is highly correlated with conventional measures of conditional instability. It has also been shown that changes of the reference state are highly correlated with changes of the observed GATE soundings. This suggests that the tropical atmosphere is forced to remain close to the reference state. The agency responsible for enforcing this is, presumably, cumulus convection.

This paper raises a number of questions that are left for the future. For example:

- For each observation time, what mass exchanges are required to reach the reference state? To answer this question, the nonlinear optimization problem discussed at the end of section 5 must be solved.
- What time changes of the GCAPE and the reference state would occur if the observed large-scale circulations acted alone, without compensating cumulus effects? How do these hypothetical changes in the GCAPE compare to those that actually occur?
- As discussed by L78, the global reference state used in the definition of the MAE is, in general, horizontally inhomogeneous; both saturated and unsaturated air can occur on each pressure surface. In the context of GCAPE, is it useful to allow the reference state to be horizontally inhomogeneous? As noted in sections 3 and 4, in applying the penetrator algorithm we have assumed that the enthalpy of each grid cell can be obtained from the average entropy and moisture content of the cell. In reality, a cell may contain both saturated and unsaturated volumes, e.g., if it has received an injection of cloudy air from a lower level. These two volumes will generally have distinct entropies and total mixing ratios. Since the enthalpy is a nonlinear function of the entropy and the total mixing ratio, the average enthalpy of the cell is not the same as the enthalpy based on the average entropy and the average total mixing ratio. This means that the fraction of each cell that is occupied by cloudy air will influence the total enthalpy of the cell and, therefore, the total enthalpy of the air column. It also means, interestingly, that the reference state corresponds to a certain cloud amount at each level.
- How do the results change if the penetrators are endowed with various properties? For example, we might choose to give up the assumption of adiabatic reversible mass transfer and allow a process in which some of the water vapor that is condensed inside penetrators precipitates out. This irreversible process would avoid the unrealistically large liquid water concentrations that appear in the "exact" reference state. One way of thinking about this possibility is that the physical system *tries* to attain the reference state but cannot actually do so because irreversibility inevitably creeps in.
- Besides the absolute minimum of H that denotes the reference state, do local, relative minima ever occur in the mass-exchange space? Imagine a plot like panel b of Fig. 8, but with two well-separated minima, one of which is deeper than the other. Can such a thing happen?

The penetrator algorithm discussed in section 5 bears a strong resemblance to the mass-flux methods that have been developed for use in cumulus parameterizations (e.g., Arakawa and Schubert 1974). It is interesting that such methods arise naturally in an attempt to evaluate the GCAPE. Our results encourage us to believe that it may be possible to develop a cumulus parameterization based on the concept of GCAPE and the associated reference state. Several existing cumulus parameterizations are based on the concept of adjustment towards an equilibrium sounding (Manabe 1965; Arakawa and Schubert 1974; Betts and Miller 1986; also see Arakawa and Chen 1987). The trick, of course, is to identify the equilibrium sounding. Existing parameterizations do so using simple cloud models (Arakawa and Schubert 1974) or empirical assumptions (Betts and Miller 1986).

In some parameterizations (Manabe 1965; Arakawa and Schubert 1974), but not all (Betts and Miller 1986), the equilibrium state is assumed to be one in which little or no buoyancy can be realized by a lifted parcel; in the present context this would correspond to a sounding with no GCAPE, i.e., the reference state. There is considerable empirical evidence that the convective atmosphere is prevented from attaining a high degree of conditional instability (e.g., Lord and Ar-

akawa 1982; Xu and Emanuel 1989). It is natural to suppose that Lorenz's reference state represents a suitable equilibrium sounding towards which a cumulus parameterization might "adjust."

The results presented in section 2 provide evidence for this idea. In particular, we note the "closeness" of the observed GATE soundings to the corresponding reference soundings and, more importantly, the strong temporal correlation between the reference state and the given state, as revealed by Figs. 5 and 6. This correlation suggests that these two states are coupled together by a very efficient and "fast" physical process, which, we assert, is cumulus convection.

The appeal of this concept is that Lorenz's reference state can be found from first principles without cloud models or empirical assumptions. This suggests that a cumulus parameterization based on the concept of GCAPE might be relatively simple and relatively free from questionable modeling assumptions.

Acknowledgments. Dr. Kuan-Man Xu's thorough and constructive review led to substantial improvements in the final version of this paper. We are indebted to Professor Richard Reed for allowing us to use the GATE data as analyzed by his group. Support has been provided by the National Science Foundation under Grant ATM-8907414 to Colorado State University. Computing resources were provided by the National Center for Atmospheric Research.

APPENDIX A

Thermodynamic Formulas

The purpose of this appendix is to summarize the thermodynamic formulas that were actually used. Further details, including derivations of some of the equations, can be found in L79.

As input, the temperature and total mixing ratio of water were read as functions of pressure. We thus have a list of parcels, each of which resides in the given state at a certain pressure with a certain temperature and a certain mixing ratio. For simplicity, the pressures are equally spaced.

Next, the entropy and enthalpy of each parcel are determined, using

$$(1 + \bar{w})s = (c_p + \bar{w}c_{pw}) \ln T - R \ln(p - e) - \bar{w}R_w \ln e - (\bar{w} - w)L/T, \quad \text{(A.1)}$$

$$(1 + \bar{w})h = (c_p + \bar{w}c_{pw})T - (\bar{w} - w)L, \quad \text{(A.2)}$$

where $\bar{w}$ is the total mixing ratio of water (liquid plus vapor), s is the entropy per unit mass, c_p is the specific heat at constant pressure of dry air, c_{pw} is the specific heat at constant pressure of water vapor, T is the temperature, R is the gas constant for dry air, p is the pressure, e is the partial pressure of water vapor, R_w is the specific gas constant for water vapor, w is the mixing ratio of water vapor, L is the latent heat of condensation, and h is the enthalpy per unit mass. Note that (A.1)–(A.2) are identical to (15)–(16) of L79, except that (15) of L79 contains a typographical error. [In the first term of the second line of L79's Eq. (15), w is written in place of $\bar{w}$.] An explanation of (A.1)–(A.2) is given by L79. Since T, p, and $\bar{w}$ are known, evaluation of w, $L(T)$, and e is straightforward. At the same time, the parcel's saturation temperature and pressure are determined (Betts 1982).

When a parcel is displaced, it strictly conserves its entropy and total mixing ratio, as well as its saturation temperature and pressure. When it arrives at a new pressure, its new enthalpy can be determined as follows. If it is placed at a pressure greater than its saturation pressure, then it is unsaturated, so that $\bar{w} = w$, and e can be determined from

$$e = \frac{wp}{\epsilon + w}, \quad \text{(A.3)}$$

where $\epsilon = R/R_w$. If it is displaced to a pressure less than its saturation pressure, then $\bar{w} > w$, and T, w, and e must be determined iteratively. As a first guess, assume that T is equal to the saturation temperature. This assumed temperature can be used to evaluate e and w. Then (A.1) is used to find a provisional value of the entropy, here denoted by $\hat{s}$ and also $(\partial s/\partial T)_p$. A correction to the temperature is then obtained from

$$\Delta T = \frac{s - \hat{s}}{(\partial s/\partial T)_p}. \quad \text{(A.4)}$$

The iteration is repeated until ΔT is sufficiently small, at which point T, w, and e have been determined with sufficient accuracy. Then the enthalpy is evaluated from (A.2).

Finally, the virtual temperature must be determined. This is obtained from

$$T_v = T\left(\frac{1 + w/\epsilon}{1 + \bar{w}}\right). \quad \text{(A.5)}$$

Recently we have generalized our thermodynamic equations to allow for the effects of ice, following the approach of Ooyama (1990). Discussion of this straightforward change will be given elsewhere.

APPENDIX B

A Parcel-moving Algorithm

The parcel-moving algorithm described here is a modified version of that given by L79. Our goal is to find the pressure at which each parcel resides in the reference state. We begin by determining which parcel resides at the lowest pressure in the reference state, then consider the second-lowest pressure, and so on, until all parcels have been assigned reference-state pressures. Lorenz's parcel-moving algorithm is based on the simple fact that the virtual potential temperature cannot decrease upward in the reference state.

TABLE 6. Reference sounding determined with the test suggested by Lorenz for GATE observation time 71. Here RH denotes the relative humidity. The corresponding correct results are given in Table 1.

Level	p (mb)	T (K)	$\bar{w}$ (g kg^{-1})	RH (%)	θ_v (K)	$\bar{w} - w$ (g kg^{-1})	$T_R - T$ (K)	$\bar{w}_R - \bar{w}$ (g kg^{-1})
1	112.5	197.3	0.008	67.7	368.3	0.00	0.0	0.0
2	137.5	201.6	0.008	41.3	355.2	0.00	0.0	0.0
3	162.5	207.3	0.014	40.1	348.3	0.00	0.0	0.0
4	187.5	218.8	17.05	13 221.0	347.1	16.92	5.5	17.0
5	212.5	225.7	16.82	6 716.4	345.6	16.57	6.0	16.8
6	237.5	228.2	0.028	9.5	344.1	0.00	2.4	−0.1
7	262.5	237.6	16.60	2 356.5	342.8	15.90	5.9	16.5
8	287.5	239.5	0.051	6.6	342.0	0.00	2.4	−0.2
9	312.5	244.3	0.096	8.5	340.6	0.00	2.2	−0.2
10	337.5	248.9	0.130	8.2	339.4	0.00	2.5	−0.2
11	362.5	253.4	0.223	10.1	338.6	0.00	3.1	−0.2
12	387.5	257.5	0.285	9.8	337.6	0.00	3.5	−0.3
13	412.5	260.9	0.335	9.2	336.1	0.00	3.6	−0.6
14	437.5	264.1	0.422	9.5	334.5	0.00	3.7	−0.9
15	462.5	267.1	0.612	11.7	333.0	0.00	4.8	−1.4
16	487.5	269.9	0.931	5.0	331.5	0.00	4.9	−2.0
17	512.5	272.4	1.338	18.8	323.0	0.00	5.4	−2.4
18	537.5	274.5	1.972	25.1	328.1	0.00	5.5	−2.6
19	562.5	276.1	2.946	34.9	326.0	0.00	5.4	−2.3
20	587.5	277.7	3.774	41.7	323.9	0.00	5.1	−2.0
21	612.5	279.2	4.578	47.4	322.0	0.00	4.6	−1.8
22	637.5	280.6	5.225	51.1	320.0	0.00	4.0	−2.0
23	662.5	282.0	5.806	53.4	318.3	0.00	3.6	−1.8
24	687.5	283.8	6.329	53.6	317.0	0.00	3.5	−1.9
25	712.5	285.5	7.209	56.4	315.9	0.00	3.5	−1.6
26	737.5	287.1	7.584	55.3	314.6	0.00	3.5	−1.1
27	762.5	288.7	8.204	55.7	313.5	0.00	3.5	−0.5
28	787.5	290.2	8.766	55.9	312.3	0.00	3.7	−0.3
29	812.5	291.6	8.719	52.5	311.0	0.00	4.1	−0.5
30	837.5	292.9	8.730	49.6	309.8	0.00	4.4	−1.9
31	862.5	294.0	8.456	46.3	308.2	0.00	4.3	−3.1
32	887.5	294.8	9.172	49.1	306.7	0.00	3.7	−3.5
33	912.5	295.7	10.67	55.6	305.5	0.00	3.1	−2.8
34	937.5	296.7	11.51	57.9	304.3	0.00	2.6	−3.2
35	962.5	298.0	12.63	60.5	303.5	0.00	2.3	−4.0
36	987.5	299.3	13.45	61.0	302.8	0.00	1.8	−3.4
37	1006.2	300.1	14.73	64.9	302.2	0.00	1.3	−2.3

Although this fact is intuitively obvious, its proof, based on the thermodynamic relations given in appendix A, is worth outlining. The first law of thermodynamics can be written in the form

$$dh = Tds + \alpha dp. \qquad \text{(B.1)}$$

A parcel that is adiabatically displaced to a lower pressure (i.e., with $ds = 0$) thus experiences a decrease in its enthalpy proportional to the product of the pressure decrease and its specific volume.

Using the methods of appendix A, the virtual temperature of a parcel can be determined as a function of its entropy, total mixing ratio, and pressure. The sounding consists of a set of parcels with certain entropies and total mixing ratios. Each parcel is assigned to a certain pressure level. Let p_A be the lowest pressure in the sounding (the "top" pressure level), and let p_B be the highest pressure in the sounding (the "bottom" pressure level). Let the virtual temperatures obtained for parcel k at pressures p_A and p_B be denoted $T_{vA}(k)$ and $T_{vB}(k)$, respectively. As discussed by L79, the parcel that resides at p_A in the reference state must be *either* the one with the highest $T_{vA}(k)$ *or* the one with the highest $T_{vB}(k)$.

To decide which, L79 suggested the following test. Consider two states:

1) The parcel with the highest $T_{vA}(k)$ is placed at p_A, and the parcel with the highest $T_{vB}(k)$ is placed at the first pressure level below p_A.

2) The parcel with the highest $T_{vB}(k)$ is placed at p_A, and the parcel with the highest $T_{vA}(k)$ is placed at the first pressure level below p_A.

Choose the possibility that gives the lowest total enthalpy for the two parcels under consideration. We have found that this algorithm does not necessarily lead to the lowest enthalpy state; in fact, it can actually increase the total enthalpy of the system! The reason is that the

total enthalpy of the system is not considered in the test; only the total enthalpy of the two parcels is considered.

Table 6 shows the results obtained using L79's test. Parcels 37, 36, and 35 (the lowest three parcels in the given state) rise to levels 4, 5, and 7 in the reference state. The algorithm gives the impossible result that the GCAPE is -11.46 J kg^{-1}. The corresponding correct results are given in Table 1.

We follow a slightly different approach. We compute the total enthalpy of the system for the following two states:

1) The parcel with the highest $T_{vA}(k)$ is lifted to p_A, and the intervening parcels are shifted down by one level each.

2) The parcel with the highest $T_{vB}(k)$ is lifted to p_A, and the intervening parcels are shifted down by one level each.

We choose the possibility that gives the lowest total enthalpy for the system. Obviously, this algorithm can never increase the total enthalpy of the system.

Once we have determined which parcel resides at the top pressure level in the reference state we *redefine* p_A to be the second pressure level from the top and repeat the test described above, considering all of the parcels whose reference-state pressures have not yet been identified. This process is continued until the reference-state pressures of all parcels have been determined.

REFERENCES

Arakawa, A., and W. H. Schubert, 1974: The interaction of a cumulus cloud ensemble with the large-scale environment, Part I. *J. Atmos. Sci.*, **31**, 674–701.

——, and J.-M. Chen, 1987: Closure assumptions in the cumulus parameterization problem. *Short and Medium Range Numerical Weather Prediction.* Collection of Papers Presented at the WMO/IUGG Symposium on Numerical Weather Prediction, Tokyo, 4–8 August 1986, Special Vol., *J. Meteor. Soc. Japan.*, 107–131.

Betts, A. K., 1982: Saturation point analysis of moist convective overturning. *J. Atmos. Sci.*, **39**, 1484–1455.

——, and M. J. Miller, 1986: A new convective adjustment scheme. Part II: Single column tests using GATE wave, BOMEX, ATEX, and arctic air-mass data sets. *Quart J. Roy. Meteor. Soc.*, **112**, 693–709.

Cheng, M.-D., 1989: Effects of downdrafts and mesoscale convective organization on the heat and moisture budgets of tropical cloud clusters. Part II: Effects of convective-scale downdrafts. *J. Atmos. Sci.*, **46**, 1540–1564.

Dudhia, J., and W. M. Moncrieff, 1987: A numerical simulation of quasistationary tropical convective bands. *Quart. J. Roy. Meteor. Soc.*, **113**, 929–967.

Krueger, S. K., 1988: Numerical simulation of tropical cumulus clouds and their interaction with the subcloud layer. *J. Atmos. Sci.*, **45**, 2221–2250.

Lord, S. J., and A. Arakawa, 1980: Interaction of a cumulus ensemble with the large-scale environment. Part II. *J. Atmos. Sci.*, **37**, 2677–2692.

Lorenz, E. N., 1955: Available potential energy and the maintenance of the general circulation. *Tellus*, **7**, 157–167.

——, 1978: Available energy and the maintenance of a moist circulation. *Tellus*, **30**, 15–31.

——, 1979: Numerical evaluation of moist available energy. *Tellus*, **31**, 230–235.

Manabe, S., J. Smagorinsky, and R. F. Strickler, 1965: Simulated climatology of a general circulation model with a hydrologic cycle. *Mon. Wea. Rev.*, **93**, 769–798.

Ooyama, K. V., 1990: A thermodynamic foundation for modeling the moist atmosphere. *J. Atmos. Sci.*, **47**, 2580–2593.

Soong, S.-T., and W.-K. Tao, 1980: Response of deep tropical cumulus clouds to mesoscale processes. *J. Atmos. Sci.*, **37**, 2016–2034.

Thompson, R. M., S. W. Payne, E. E. Recker, and R. J. Reed, 1979: Structure and properties of synoptic scale wave disturbances in the intertropical convergence zone of the eastern Atlantic. *J. Atmos. Sci.*, **36**, 53–72.

Xu, K.-M., 1991: The coupling of cumulus convection with large-scale processes. Ph.D. thesis, University of California, Los Angeles, 250 pp.

——, and K. A. Emanuel, 1989: Is the tropical atmosphere conditionally unstable? *Mon. Wea. Rev.*, **117**, 1471–1479.

Yanai, M., S. K. Esbensen, and J.-H. Chu, 1973: Determination of bulk properties of tropical cloud clusters from large-scale heat and moisture budgets. *J. Atmos. Sci.*, **30**, 611–627.